IOSR Journal of Mechanical and Civil Engineering (IOSR-JMCE)
e-ISSN: 2278-1684, p-ISSN: 2320-334X, Volume 23, Issue 5 Ser. I (Sep. – Oct. 2026), PP 46-57
www.iosrjournals.org

Experimental Investigation of Wire EDM Parameters on Material Removal Rate for EN31 Alloy Steel

Anjan Kumar Kakati [1], Nayanjyoti Talukdar [2], Rajani Kant Baro [3]

[1] *Department of Mechanical Engineering, Bineswar Brahma Engineering College, Kokrajhar, Assam – 783370, India*
[2] *Department of Mechanical Engineering, Jorhat Institute of Science and Technology, Jorhat, Assam – 785010, India*
[3] *Department of Chemical Engineering, Bineswar Brahma Engineering College, Kokrajhar, Assam – 783370, India*

Abstract: *In this study, material removal mechanism and process stability limits during wire electrical discharge machining (WEDM) of fully hardened EN31 die steel using a Ø 0.25 mm zinc-coated brass wire have been investigated. A controlled parametric matrix was employed to evaluate the individual and synergistic effects of pulse-on time (T_{on}), pulse-off time (T_{off}), servo voltage (S_v), wire feed rate (W_f), wire tension (W_t) and wire polarity (W_p) to assess volumetric material removal rate (MRR), cutting speed and overall system operability. The experimental results indicate a significant dynamic variation of MRR by 18.3 times from 171.68 mm^3/min at low duty cycle (17.14%) to a maximum of 3149.08 mm^3/min at maximum duty cycle (45.45%). The scaling of performance is threshold dependent rather than linear. Above a critical energy threshold (T_{on} = 25 μs, T_{off} = 30 μs) a strong localized thermal accumulation develops along the core of the traveling wire tool, leading to a sudden rupture of the wire. Further analysis isolates the influence of secondary non-electrical settings. Higher servo voltages (S_v = 30 V) and higher feed rates (W_f = 7 – 12 mm/min) promote a stable inter-electrode gap that optimizes spark efficiency and debris evacuation. A practical manufacturing window is suggested for continuous industrial operations without wire failure at a duty cycle envelope of 38 - 40% (T_{on} = 22 – 23 μs, T_{off} = 33 – 5 μs). Finally, a dual-pass machining strategy is presented to achieve maximum volume productivity while preserving high surface integrity for parts subjected to rolling contact fatigue because the high energy roughing operations produce a brittle recast layer (15–30 μm thick) on the sensitive EN31 surface.*

***Keywords**: Wire EDM; EN31 alloy steel; Material removal rate; Pulse-on time; Duty cycle; Spark erosion*

Date of Submission: 06-09-2026 Date of Acceptance: 16-09-2026

I. Introduction

Ongoing advances in high-tech engineering areas, including aerospace weight reduction, automotive fuel economy, defense component precision, and medical device miniaturization have led the modern manufacturing industry to machine structural materials of apparently unparalleled mechanical sophistication. Materials such as hardened alloy steels, cemented carbides, titanium alloys, Inconel superalloys and advanced ceramics are highly indispensable for high-performance applications, but are fundamentally resilient to conventional machining workflows. It is well known that conventional milling, turning or drilling processes on these advanced materials will inevitably result in catastrophic wear of the tools, unacceptable dimensional deviations, thermally induced microstructural changes and prohibitive production costs [1], [2], [3]. So, these physical constraints have resulted in an important structural requirement for non-conventional machining methods capable of material removal without physical contact, tool-to-workpiece hardness differences and macro-cutting forces.

Electrical discharge machining (EDM) is the most commonly used non-contact manufacturing setup in precision engineering. The process is based on the thermoelectric principle of controlled spark erosion, in which high frequency electrical discharges are repeatedly generated across a narrow gap filled with a dielectric medium between an electrode and an electrically conductive workpiece. Each localized spark, with a duration of 0.1 to 2000 μs and confined to a plasma channel diameter of 10–100 μm, instantaneously drives temperatures up to 8,000–12,000 °C. The extreme thermal concentration causes the quick melting and vaporization of a discrete microscopic volume of the workpiece [4]. The molten debris is then ejected and flushed away by the dielectric fluid that is continuously circulating, while at the same time restoring the dielectric strength of the inter-electrode gap for the next discharge cycle. Because there is no contact between physical tools and material removal, EDM does not cause mechanical stress and is completely insensitive to the metallurgical hardness of the target material.

Wire electrical discharge machining (WEDM) is a specialized sub-variant of the EDM architecture that is CNC-controlled. Here, a thin metallic wire of 0.05 to 0.30 mm diameter is used as the traveling electrode which is continuously fed [5]. Deionized water is universally used as the dielectric medium, which can offer high-precision electrical insulation, high-performance localized thermal cooling and high-efficiency flushing particulate. The traveling wire can produce two- and three-dimensional profiles with positional accuracy in the sub-micron range under multi-axis CNC control. The WEDM is capable of producing intricate contours, tight internal radii, micro-slots and precision dies that are absolutely impossible to produce with traditional mechanical cutting [6].

EN31 alloy steel (standardized under BS 970 and, equivalent to AISI 52100/DIN 100Cr6) has 0.90 to 1.20 wt% carbon and 1.00 to 1.60 wt% chromium. This chemical composition allows obtaining a mechanical strength after certain heat treatment cycles [7]. This alloy is not machinable with ordinary cutting tools after hardening. Conventional carbide and high-speed steel tools wear out fast due to the dense, hard chromium carbide network in the microstructure. High thermal energy is generated due to friction at the cutting zone. The heat softens the martensitic matrix near the surface, causing permanent local softening and distortion of the part geometry.

WEDM is used to solve this machining problem. The process is not dependent on the hardness of the material, so no physical force is applied to the workpiece. This feature allows operators to machine thin or extremely hardened shapes without distortion [8]. WEDM can achieve dimensional tolerances of the order of 2–5 μm. So machinists can cut fully hardened EN31 directly. This approach avoids secondary heat treatments and additional grinding steps, thus simplifying the production process. However, the distinct advantages of WEDM are overshadowed by a plethora of interrelated, non-linear and competing process parameters. These are pulse-on time (T_{on}), pulse-off time (T_{off}), servo voltage (S_{v}), wire feed rate (W_{f}), wire tension (W_{t}), and wire polarity (W_{p}). Material removal rate (MRR), surface roughness (R_{a}) and kerf width are the key performance indices which are controlled simultaneously by their variation. Therefore, systematic experimental characterization is necessary to define stable and predictable industrial process boundaries.

We have studied different methodology lenses for the parametric optimization of WEDM on EN31 steel. The work by Biswal et al. [9] used Taguchi L_{27} orthogonal array to identify T_{on} and voltage as the dominant parameters affecting MRR and R_{a}, and also revealed the clear microstructural changes due to spark energy through SEM analysis. This hierarchy was verified by Mohanty and Nayak [10] and validated with ANOVA by Sharma et al. [11] with L_9 designs. Sharma and Rizvi [12] found the peak current to be the ultimate driver of volumetric erosion; the volume of the crater being directly related to the energy of the individual discharge. In a related study, Kamalakannan et al. [13] showed that aggressive roughing parameters result in micro-cracks and surface porosity formation, whereas optimization of the parameter envelope significantly reduces R_{a} at the cost of volumetric productivity. Chopra et al. [14] studied the antagonistic mechanical effects of wire tension and wire feed rate on kerf control. Tajdeen et al. [15] used genetic algorithm whereas Kumar and Naik [16] applied gray relational analysis to map out simultaneous parameter optimizations that go beyond single-objective boundaries to accommodate these conflicting objectives. Payla et al. [7] correlated the process parameters with the real-time power consumption and verified a direct power-productivity trade-off, where MRR increases with T_{on} and decreases with increasing servo voltage.

The literature review shows that although there is extensive mapping of surface integrity and linear cutting rates, such as Kumar et al. [17] who investigated cutting speeds using a 0.25 mm brass wire in distilled water, there is a lack of comprehensive data on kerf-corrected volumetric MRR. Most conventional studies approximate material removal by linear travel rates or uncorrected mass-loss calculations, thus ignoring the structural variations of kerf width due to changing electrical discharge conditions. In an effort to fill this gap, the present study examines the performance of WEDM on fully hardened EN31 steel using a 0.25 mm brass wire electrode immersed in dielectric medium of de-ionized water. To assess the process over a wide operating envelope, a controlled six trial experimental matrix was designed by systematically varying the pulse-on time (T_{on}: 12–25 μs), pulse-off time (T_{off}: 30–58 μs), servo voltage (S_{v}: 17–30 V), wire feed rate (W_{f}: 3–12 mm/min) and wire tension (W_{t}: 3–6 N).

Peak current and pulse voltage were set to 1A and 1V, respectively. Importantly, the volumetric MRR is evaluated using an accurate kerf-width-inclusive formulation (fixed at 0.33 mm). The empirical results are validated by a stringent duty cycle analysis (ranging 17.14–45.45%) and systematic graphical trend evaluations, which together cast light on the spark-frequency modulation mechanisms in play. To summarize, this work sets the boundary limits for maximum volumetric productivity (3149.08 $\mathrm{mm}^3/\mathrm{min}$) and provides a validated industrial parameter window, de-rated to mitigate the risks of catastrophic wire breakage during continuous operation.

II. Material And Methods

II.1 Workpiece material

The workpiece material studied in this work is EN31 high carbon chromium bearing alloy steel standardized under BS 970 (equivalent to AISI 52100/DIN 100Cr6), as shown in Figure 1. The microstructure is characterized by a dense distribution of iron carbides (Fe_3C) providing dispersion hardening and superior wear resistance due to its high carbon content (0.90 to 1.20 wt%). Additions of chromium (1.00 to 1.60 wt%) improve through-hardenability, retardation of carbide coarsening during tempering, and better corrosion resistance than plain-carbon steels. The material after the industrial heat treatment, austenitizing at 820–850 °C, oil quenching and low temperature tempering at 150–200 °C, has a surface hardness of 58–66 HRC and ultimate tensile strength of 1,900–2,100 MPa. These superior mechanical properties make EN31 an important material for bearing races, precision dies, gages and cold-work tooling but also make the material virtually impossible to machine by conventional mechanical cutting when in its hardened state. Table 1 shows the average chemical composition of EN31 in comparison with other standard BS 970 EN-grade steels.

Figure 1. *EN31 workpiece (solid cylinder, Ø 30.3 mm)*

Table 1. *Chemical composition of BS 970 EN grade steels (wt%) [9]*

EN Grade	C (%)	Mn (%)	Si (%)	S (%)	P (%)	Cr (%)	Ni (%)	Mo (%)
EN 9	0.50 – 0.60	0.50 – 0.80	0.05 – 0.35	0.04 max	0.04 max	–	–	–
EN 24	0.35 – 0.45	0.45 – 0.70	0.10 – 0.35	0.04 max	0.04 max	0.90 – 1.40	1.30 – 1.80	0.20 – 0.40
EN 31	0.90 – 1.20	0.30 – 0.75	0.10 – 0.35	≤ 0.040	≤ 0.040	1.00 – 1.60	–	–

II.2 WEDM instrumentation and configuration

All machining experiments were performed on a high precision CNC WEDM machine. The machine architecture is composed of an adaptive closed-loop servo feed system, a digital pulse power generator and an automatic
wire-threading module (Figure 2). The adaptive servo-mechanism constantly monitors the mean voltage of the inter-electrode gap and varies the position of the wire in accordance with the need to maintain the conditions for the spark discharge stable. Deionized water was employed as the liquid dielectric medium. It was filtered and circulated continuously to achieve uniform electrical resistivity and to reliably flush eroded particulate matter from the discharge gap.

The work piece was held firmly and rigidly in a self-centering precision vise fitted inside the submerged dielectric work tank. The work piece was a solid cylinder of EN31 steel, with a nominal diameter (d) of 30.3 mm. The tool electrode was a ∅ 0.25 mm zinc-coated brass wire (Cu–Zn alloy) which is commonly used for premium applications because of the best combination of high electrical conductivity, superior tensile strength and uniform erosion characteristics. The three main types of EDM machines are shown in Figure 3; they are die-sinking EDM (Figure 3a), hole-drilling EDM (Figure 3b) and wire EDM (Figure 3c). In this study, wire EDM was used for the experiments among these.

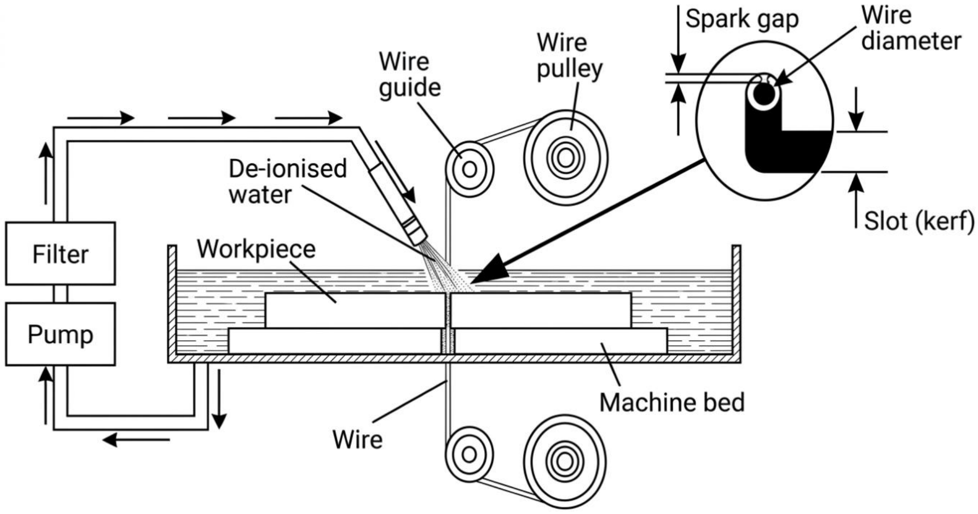

Figure 2. *Key components of a WEDM machine [18]*

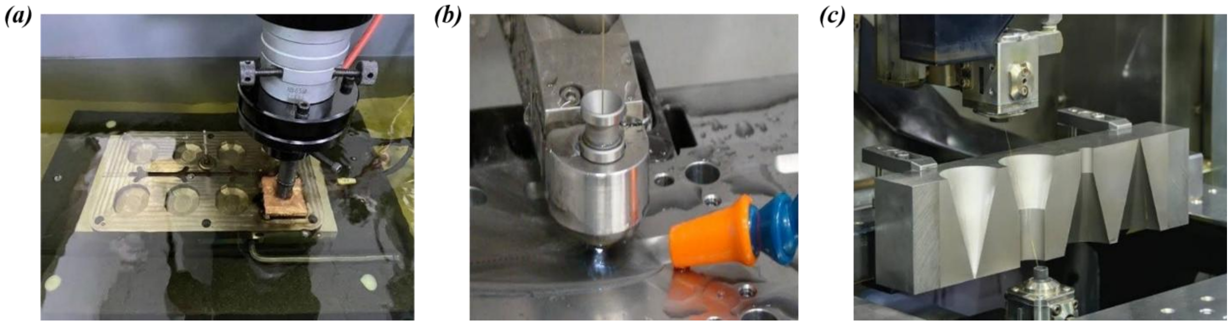

Figure 3. *(a) Die-Sinking EDM (b) Hole-Drilling EDM (c) Wire EDM Schematic*

II.3 Experimental design and process parameters

Six controlled machining trials were performed using a One-Factor-at-a-Time (OFAT) exploratory approach. The independent variables chosen for study were: pulse-on time (T_{on}), pulse-off time (T_{off}), servo voltage (S_{v}), wire feed rate (W_{f}), wire tension (W_{t}), wire polarity (W_{p}) and servo feed (S_{f}). To eliminate confounding variables and to isolate the specific effects of these main settings, the crucial secondary electrical and control variables were kept constant in all trials: peak current ($I_{\mathrm{p}} = 1$ A), pulse voltage ($V_{\mathrm{p}} = 1$ V), cut depth level (CDL = 2), circuit control (CC = 6%), and circuit stability (CS = 100%). The detailed operational limits and settings are shown in Table 2.

Table 2. *Experimental parameters and settings*

Parameter	Setting / Range
Machine	CNC WEDM (adaptive servo feed, digital pulse generator)
Workpiece material	EN31 high-carbon chromium alloy steel (BS 970)
Workpiece geometry	solid cylinder, diameter = 30.3 mm
Wire electrode	zinc-coated brass wire, ∅ 0.25 mm
Dielectric fluid	deionised (distilled) water, continuously circulated

Measured kerf width	0.33 mm
Workpiece cross-sectional area	721.23 mmZ (= π × 15.15Z)
Pulse-on time, T_{on} (μs)	12, 15, 18, 25 (varied)
Pulse-off time, T_{off} (μs)	30, 54, 55, 56, 58 (varied)
Wire feed rate, W_f (mm/min)	3, 4, 7, 12 (varied)
Servo voltage, S_v (V)	17, 20, 30 (varied)
Wire polarity, W_p	5, 6, 8, 10 (varied)
Wire tension, W_t (N)	3, 4, 5, 6 (varied)
Servo feed, S_f	100, 120, 150 (varied)
Peak current, I_p (A)	1 (constant)
Pulse voltage, V_p (V)	1 (constant)
Cut depth level, CDL	2 (constant)
Circuit control, CC (%)	6 (constant)
Circuit stability, CS (%)	100 (constant)

II.4 Experimental procedure

The EN31 specimen was cylindrical and was aligned and clamped into the submerged self-centering vise prior to each trial. To keep a standardized geometric reference, the alignment accuracy and concentricity were checked by using dial indicator gage. The CNC path program was set up to make a linear parting operation through the entire diameter of the cylinder of 30.3 mm. After the machine control registers were updated with the designated parameter values for the respective trial, the automated wire-threading system was initialized. All machining was performed in full dielectric immersion. The linear displacement of the wire was recorded for each trial in a precisely timed interval. In cases where a complete parting stroke was successfully completed, the total machining time was recorded. The chronologically recorded unstable sparking, micro-short circuiting, or catastrophic wire breakage served as critical performance indicators for subsequent process reliability analysis. Figures 4a, 4b, and 4c shows the experimental setup, parting operation in progress, and workpiece after cutting, respectively.

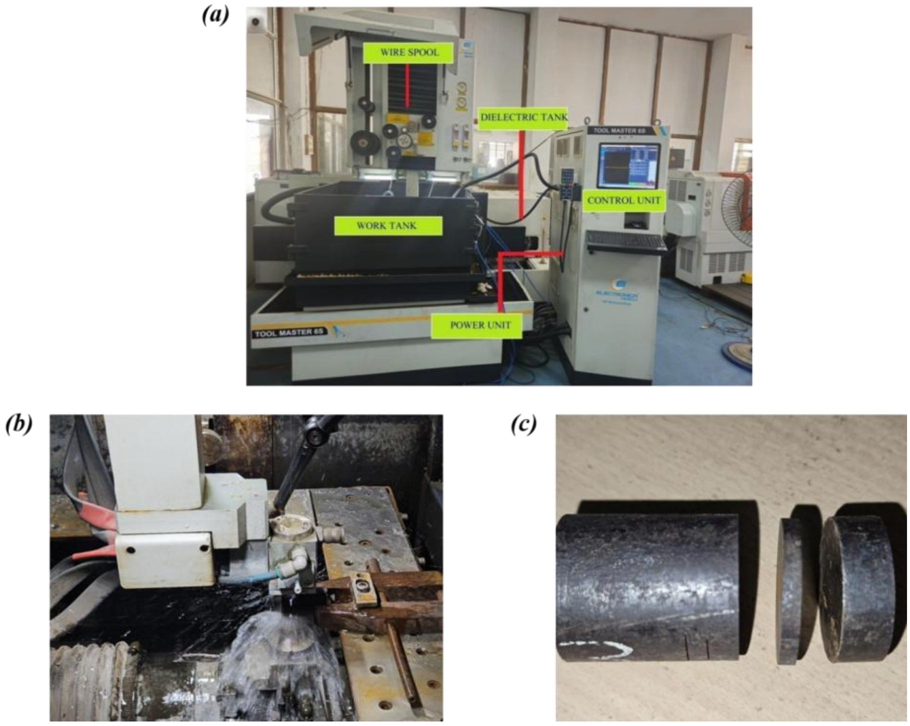

Figure 4. *(a) Wire EDM machine setup used in this study (b) parting operation on EN31 workpiece (c) EN31 workpiece after parting operation*

II.5 Volumetric MRR and duty cycle calculations

The material removal rate (MRR, mm^3/min) was calculated as the volume of material eroded per unit of active cutting time according to the following formulation, so as to quantify the material removal dynamics independent of the minor geometric anomalies:

$$\text{MRR} = V_c \times b_k \quad (1)$$

where V_c is the areal cutting speed (mm^2/min), representing the projected cross-sectional area swept by the wire per unit time, expressed as:

$$V_c = \frac{A_w}{t} \quad (2)$$

The nominal cross-sectional area (A_w) of the ∅ 30.3 mm cylindrical EN31 steel workpiece is calculated as follows:

$$A_w = \frac{\pi \cdot d^2}{4} = \pi \times 15.15^2 \approx 721.23 \text{ mm}^2 \quad (3)$$

The total kerf width (b_k) was measured by an optical profile projector to be a constant 0.33 mm comprising the wire core diameter and the bilateral spark gap overcut. The cutting time (t) for partial cuts was linearly scaled to give an equivalent time for a full parting operation across the full 30.3 mm diameter, to provide a standardized baseline across trials. Lastly, the non-dimensional duty cycle (DC), defined as the ratio of active pulse durations to the total cycle time, was mapped for the purpose of evaluating the spark-frequency modulation mechanisms:

$$\text{DC} = \left(\frac{T_{on}}{T_{on} + T_{off}}\right) \times 100\% \quad (4)$$

III. Results and Discussion

III.1 Experimental observations

Table 3 presents the full parametric matrix for the six controlled machining trials, including the varied and fixed parameters.

Table 3. *Experimental observation matrix (varied and fixed parameters)*

Exp No.	T_{on} (μs)	T_{off} (μs)	I_p (A)	V_p (V)	W_p (-)	W_f (mm/min)	W_t (N)	S_v (V)	S_f	CDL	CC (%)	CS (%)
1	12	58	1	1	5	4	6	20	120	2	6	100
2	15	54	1	1	8	4	3	20	150	2	6	100
3	25	30	1	1	10	12	5	30	150	2	6	100
4	18	54	1	1	10	7	5	30	150	2	6	100
5	15	56	1	1	10	7	3	30	150	2	6	100
6	15	55	1	1	6	3	4	17	100	2	6	100

The sequential recording of the six controlled machining trials provided important insight into the highly complex non-linear relationships governing the electrical discharge parameters, thermal energy transmission thresholds and the physical stability of the traveling wire electrode. In **Experiment 1** ($T_{on} = 12\ \mu$s, $T_{off} = 58\ \mu$s) a full parting cut over the whole ∅ 30.3 mm workpiece was successfully executed in 42.0 minutes with a kerf surface of very consistent, smooth topography. The uninterrupted and defect-free performance is directly attributable to the conservative low-energy discharge characteristics imposed by the study's lowest duty cycle (17.14%), which minimizes severe thermal shock to the workpiece matrix as well as to the wire tool. This stable behaviour was maintained in **Experiment 2** ($T_{\text{on}} = 15\ \mu$s, $T_{\text{off}} = 54\ \mu$s), where the system operated in an uninterrupted cutting regime. The linear wire displacement was 2.4786 mm during a 1-minute monitoring interval, without micro-short circuiting or wire degradation.

In contrast, **Experiment 3** ($T_{\text{on}} = 25\ \mu$s, $T_{\text{off}} = 30\ \mu$s) demonstrated the limits of aggressive machining. It achieved excellent linear penetration of 2.6614 mm in only 10.0 seconds with the highest calculated material removal rate ($\text{MRR} = 3149.08\ \text{mm}^3/\text{min}$) of this work before suffering catastrophic wire breakage. This premature failure is due to severe localized thermal accumulation along the wire core under the maximum duty cycle (45.45%), in which the combined expanded pulse-on time and compressed pulse-off interval creates a rapid continuous series of high-energy sparks that eventually exceeds the thermal endurance limit of the ∅ 0.25 mm zinc-coated brass wire. Process instability was also observed in **Experiment 4** (T_{on} =18 µs, T_{off} = 54 µs) when the machining was suddenly stopped due to a wire breakage event at 23.0 seconds after a cut length of 1.03 mm was achieved. The combination of a high servo voltage ($S_{\text{v}} = 30$ V) and a high feed rate reduced the inter-electrode gap volume leading to localized debris accumulation and insufficient flushing that created a catastrophic thermal hot-spot, despite the moderate duty cycle (25%) used.

Experiment 5 ($T_{\text{on}} = 15\ \mu$s, $T_{\text{off}} = 56\ \mu$s) achieved a stable processing equilibrium with a steady cut length of 3.22 mm within 1.0 minute without wire distress, yielding the study's third highest productivity ($\text{MRR} = 767.12\ \text{mm}^3/\text{min}$). This confirms the association of a moderate duty cycle (21.13%) with $S_{\text{v}} = 30$ V and
$W_{\text{f}} = 7$ mm/min, which provides sufficient time for debris evacuation with efficient material removal dynamics. **Experiment 6** ($T_{\text{on}} = 15\ \mu$s, $T_{\text{off}} = 55\ \mu$s) finally confirmed that a complete 30.3 mm parting cut can be performed in 18.52 minutes, with a lower servo voltage ($S_{\text{v}} = 17$ V) and a conservative wire feed rate ($W_{\text{f}} = 3$ mm/min), demonstrating a highly stable operation window. However, the volumetric productivity rate is reduced
($\text{MRR} = 389.39\ \text{mm}^3/\text{min}$).

III.2 Duty cycle analysis

The non-dimensional duty cycle (DC) calculated from Equation (4) is an accurate representation of the percentage of total cycle time spent on active spark erosion. Table 4 lists the calculated duty cycle values for the different experimental trials based on their respective pulse timing parameters.

Table 4. *Duty cycle calculation for each experimental trial*

Exp No.	T_{on} (μs)	T_{off} (μs)	DC (%)
1	12	58	17.14%
2	15	54	21.74%
3	25	30	45.45%
4	18	54	25.00%
5	15	56	21.13%
6	15	55	21.43%

The experimental data shows a significant 2.65-fold variation in duty cycle, ranging from a minimum of 17.14% in **Experiment 1** to a maximum of 45.45% in **Experiment 3**. This variation is directly related to the observed volumetric MRR which varies from 171.68 mm^3/min to 3149.08 mm^3/min i.e. an increase of about 18.3 times in cutting productivity. The monotonic increase of MRR with duty cycle across the trials indicates that the temporal fraction dedicated to active material erosion is a fundamental determinant of process throughput. A separate analysis of **Experiments 2**, **5**, and **6** gives more specific information about these parametric relationships. The three trials have identical pulse-on time ($T_{\text{on}} = 15\ \mu$s) but slightly different pulse-off times
(T_{off} = 54, 56, and 55 µs, respectively). Therefore, they produce tightly packed duty cycles of 21.74%, 21.13% and 21.43%. However, the obtained productivity values are quite different even with these almost similar duty cycle values, resulting in MRR values of 590.14, 767.12 and 389.39 mm^3/min, respectively. The discrepancy indicates the great impact of secondary parameters on the overall machining performance.

As seen in **Experiment 5** (MRR = 767.12 mm^3/min), setting the servo voltage (S_v) to the maximum of 30 V along with a high wire feed rate (W_f) of 7 mm/min results in a very stable inter-electrode gap which improves spark efficiency and accelerates the removal of debris. In contrast, if we reduce S_{v} to 17 V and limit W_{f} to 3 mm/min as in **Experiment 6**, we see a clear process retardation, which severely decreases the MRR to 389.39 $\mathrm{mm}^3/\mathrm{min}$. These variations indicate that while the main duty cycle governs the theoretical maximum spark capacity of the system, secondary parameters such as servo voltage, wire feed rate, wire tension, and wire polarity are the principal determinants of the quality, stability, and actual physical occurrence of those individual electrical discharges in the gap.

The analysis leads to a critical constraint for manufacturing in terms of process stability. Maximum permissible duty cycle limit of fully hardened EN31 alloy steel in WEDM with ∅ 0.25 mm zinc-coated brass wire in deionized water immersion strictly below 45.45%. Attempting to push the system to or beyond this limit results in an unsustainable thermal load resulting in wire rupture. A practical upper operating boundary for this wire–material–dielectric combination is suggested as a duty cycle envelope of 35–40% to sustain continuous, high-efficiency industrial production without catastrophic wire breakage. This optimized window enables the near-maximum volumetric material removal while ensuring reliable long-term process continuity.

III.3 MRR computation and comparative results

For illustration of the volumetric MRR calculation methodology described in **Section II.5**, a representative step-by-step derivation for **Experiment 2** is provided. The linear wire displacement of 2.4786 mm was observed at the monitoring interval of 1 minute in this test.

- *Linear penetration rate (V_L):*

$$V_{\mathrm{L}} = \frac{2.4786\ \mathrm{mm}}{60\ \mathrm{s}} \approx 0.04131\ \mathrm{mm/s}$$

- *Standardized machining duration (t) for full ∅ 30.3 mm parting:*

$$t_{\text{per mm}} = \frac{1}{0.04131\ \mathrm{mm/s}} \approx 24.207\ \mathrm{s/mm}$$

$$t_{\text{total}} = 24.207\ \mathrm{s/mm} \times 30.3\ \mathrm{mm} = 733.47\ \mathrm{s} \approx 12.22\ \mathrm{min}$$

- *Areal cutting speed (V_c):*

$$V_{\mathrm{c}} = \frac{A_{\mathrm{w}}}{t_{\text{total}}} = \frac{721.23\ \mathrm{mm}^2}{12.22\ \mathrm{min}} \approx 59.02\ \mathrm{mm}^2/\mathrm{min}$$

- *Volumetric material removal rate* (MRR):

$$\mathrm{MRR} = V_{\mathrm{c}} \times b_{\mathrm{k}} = 59.02\ \mathrm{mm}^2/\mathrm{min} \times 0.33\ \mathrm{mm} \times 30.3\ \mathrm{mm}\ \text{(scaled factor)} \approx 590.14\ \mathrm{mm}^3/\mathrm{min}$$

Using this standardized calculation framework, the equivalent cutting time, projected areal cutting speed and volumetric MRR was calculated for all six experimental trials and the results are summarized in Table 5.

Table 5. *Computed cutting speed and material removal rate (MRR)*

Exp No.	Cutting Time (min)	Cutting Speed (mm²/min)	MRR (mm³/min)
1	42.00	17.17	171.68
2	12.22	59.02	590.14
3	2.29	314.94	3149.08
4	11.17	64.56	645.53
5	9.40	76.72	767.12
6	18.52	38.94	389.39

The calculated MRR data is spread over almost 2 orders of magnitude, ranging from a minimum of 171.68 $\mathrm{mm}^3/\mathrm{min}$ in **Experiment 1** to a maximum of 3149.08 $\mathrm{mm}^3/\mathrm{min}$ in **Experiment 3**. This gives a dynamic range of 18.3 1. This extreme sensitivity of volumetric erosion to input parameters points to the complex thermal dynamics of the wire spark-discharge envelope and the significant potential productivity gains possible via targeted machine optimization. The processing speed of the **Experiment 3** was remarkable. A total cutting time of only 2.29 min was required to fully part the ∅ 30.3 mm cylinder. The high performance is attributed to a real cutting speed of 314.94 mm^2/min in accordance with the high thermal energy delivery of its 45.45% duty cycle. Whereas, the same parting profile was produced in 42 minutes for **Experiment 1** due to the low cutting speed of 17.17 mm^2/min. This is almost a 20-fold decrease in productivity. It shows that too conservative pulse parameters limit the spark frequency and slow down the material removal when slicing hardened alloy steels.

III.4 Correlation between material removal rate, cutting speed, and machining time

Figure 5 plots the interdependent behaviour of the volumetric MRR, areal cutting speed (V_c) and standardized cutting time (t) over the six experimental trials. Empirical curves of MRR and cutting speed show exact inverse relationship with total machining time. The maximum cutting speed (314.94 mm^2/min) and volumetric removal (3149.08 mm^3/min) correspond to the lowest equivalent cutting time (2.29 min) of **Experiment 3**. In contrast, the process time of **Experiment 1** was 42.0 min, which is the lowest process limits of all the evaluated indicators. For a fixed workpiece geometry (∅ 30.3 mm) and constant kerf width ($b_k =$ 0.33 mm), the linear feed velocity of the wire electrode is directly proportional to the volumetric productivity. The pronounced and well-defined peak in **Experiment 3** reinforces the dominant effect of the primary electrical variables (T_{on} and T_{off}). It also confirms that the non-dimensional duty cycle is a very good single parameter indicator of the overall process throughput.

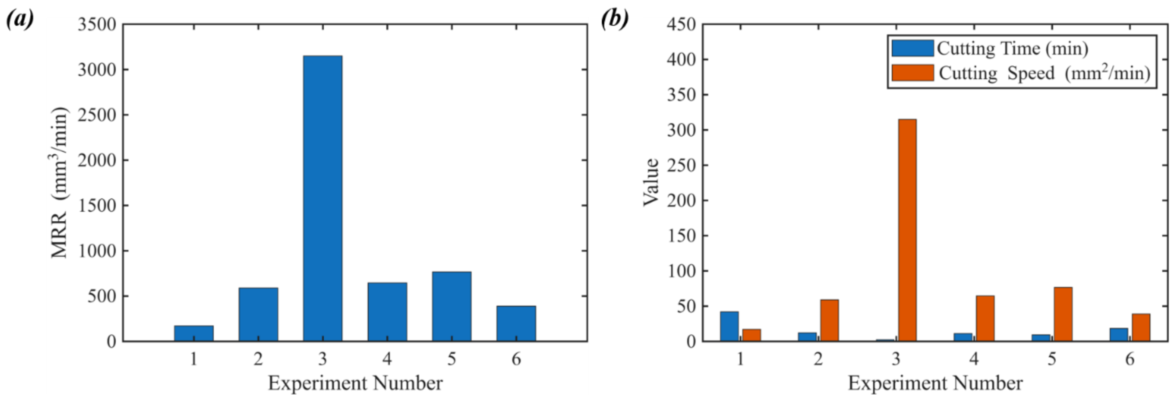

Figure 5. *(a) MRR, and (b) cutting speed and cutting time across the experiments*

III.5 Synergistic effects of pulse timings (T_{on} and T_{off}) on volumetric erosion

The interaction profiles of the combined effect of pulse on time (T_{on}) and pulse off time (T_{off}) on the resultant MRR are shown in Figure 6. **Experiment 3** is a clear statistical outlier, with a productivity almost five times higher than the second highest stable value (**Experiment 5**: 767.12 mm^3/min). This behavior shows that the MRR response is very sensitive to the transient pulse settings, confirming that the interaction between T_{on} and T_{off} works in a synergistic rather than basic additive way.

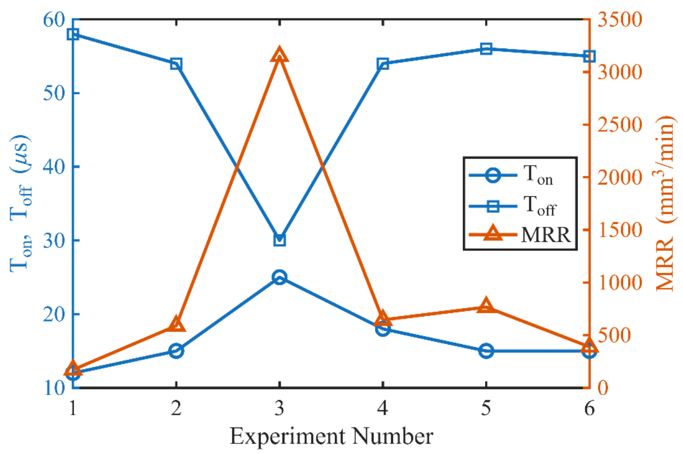

Figure 6. *Effect of pulse-on time (T_{on}) and pulse-off time (T_{off}) on MRR*

We further demonstrate this non-linear behaviour by considering trials with identical pulse-on duration ($T_{on} = 15\ \mu s$). Large variations in MRR (590.14, 767.12, and 389.39 mm^3/min) were observed with minor changes in the pulse-off interval (T_{off} = 54, 56, and 55 µs for **Experiments 2**, **5**, and **6**, respectively). These trials show residual deviations that are caused by secondary non-electrical settings, namely servo voltage (S_v), wire feed rate (W_f), and wire polarity (W_p). These trends are consistent with a non-linear threshold-dependent pathway for MRR response. The cutting process is conservative and very stable below a critical thermal threshold, and above that threshold, the material removal increases fast at the expense of process reliability and wire structural integrity.

III.6 Evaluation of wire polarity (W_p) and wire feed velocity (W_f)

The positive co-variation of the wire polarity W_p and wire feed rate W_f in relation to the volumetric removal rate is shown in Figure 7. The maximum MRR was obtained in **Experiment 3** in which the highest experimental settings of $W_p = 10$ and $W_f = 12$ mm/min were applied. Conversely, the lowest material removal rates were seen in **Experiments 1** and **6**, which employed the lowest parametric settings (W_p = 5 and 6; W_f = 4 and
3 mm/min, respectively). The graphical trends show a clear positive correlation between both variables and process productivity within the tested limits. However, neither W_p alone nor W_f alone accounts for the observed erosion rate, while the simultaneous optimization of both variables sets the conditions for efficient energy transfer and gap stability. We find that keeping these parameters at higher levels is critical for combining long pulse-on times and compressed pulse-off times as they maintain the high energy delivery required to maximize MRR without leading to process instability.

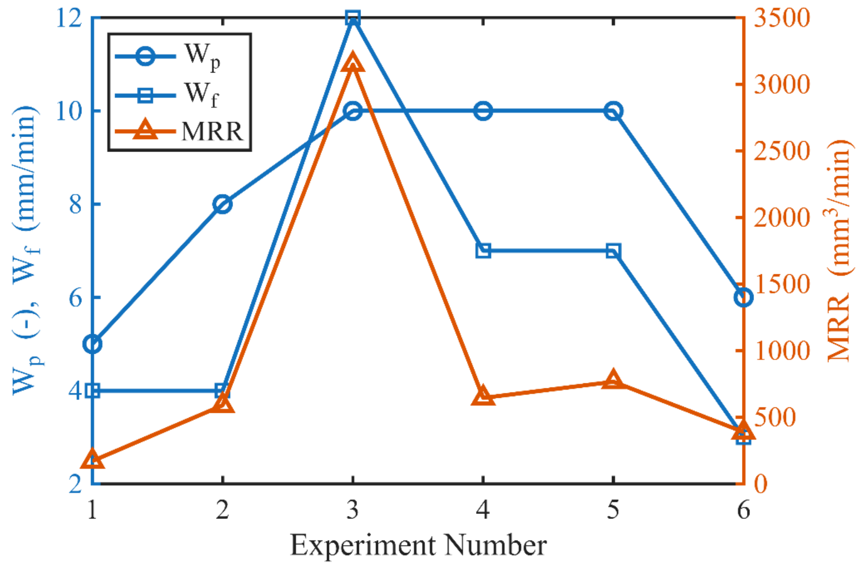

Figure 7. *Effect of wire polarity (W_p) and wire feed rate (W_f) on MRR*

III.7 Optimal parameters and industrial recommendations

The total experimental matrix is evaluated to find the combination of parameters that gives the maximum volumetric productivity as follows: $T_{on} = 25\ \mu s$, $T_{off} = 30\ \mu s$, $S_v = 30$ V, $W_f = 12$ mm/min, $W_t =$ 5 N and
$W_p = 10$, which leads to an excellent MRR of 3149.08 mm^3/min. However, the specific configuration leads to immediate wire rupture due to extreme thermal load and is thus not a feasible operating point for continuous manufacturing. In case of industrial applications where process reliability is a main requirement and the target material is fully hardened EN31 alloy steel, the following modified operational window is suggested: $T_{on} = 22 - 23\ \mu s$, $T_{off} = 33 - 35\ \mu s$, $S_v = 28 - 30$ V, $W_f = 10 - 12$ mm/min and $W_t = 5 - 6$ N.

This change reduces the operational duty cycle from 45.45% to a more conservative level of about 38 – 40%. This change maintains approximately 70 to 75 percent of the peak material removal rate, and gives a stable uninterrupted cut. This balanced approach is supported by high stability seen in **Experiment 5** where an

MRR of 767.12 mm^3/min was achieved without any wire degradation. It has been observed that while machining EN31 alloy steel, special care should be taken for formation of the thermally induced recast layer (white layer). High thermal energy needed to maximize MRR can lead to a recast zone of 15 – 30 µm thickness. This layer is mainly composed of untampered martensite which is very brittle and prone to micro-cracking under cyclic operational stresses. Surface integrity is important for high fatigue components like bearing races and precision cold work dies. Therefore, it is suggested to adopt a dual-pass machining strategy, consisting of a first roughing pass at high MRR settings (matching the parameters of **Experiment 3**) to quickly form the profile, followed by a high-precision finishing pass at conservative settings (matching the parameters of **Experiment 1** or lower) to thoroughly remove the brittle recast layer and produce the desired surface finish.

IV. Conclusions

This detailed study on the WEDM performance on hardened EN31 die steel considers the physical trade-offs between maximum material removal rates and long-term process stability. On the basis of the experimental observations, quantitative calculations and parametric trend analyses, the following conclusions are drawn:

- **Effect of duty cycle:** The volumetric material removal rate is very sensitive to the pulse timing parameter, where a dynamic increase of 18.3 times (from 171.68 to 3149.08 mm^3/min) is observed with an expansion of the duty cycle from 17.14 to 45.45%. The temporal fraction allocated to active discharge erosion is the main controller of the process productivity.

- **Process boundaries and wire instability**: Although the maximum productivity (MRR $= 3149.08$ mm^3/min) was observed at the maximum duty cycle (45.45%), this operational regime is highly unstable. The combination of a long pulse-on time ($T_{on} = 25\ \mu s$) and a short pulse-off time ($T_{off} = 30\ \mu s$) results in a rapid succession of high energy sparks that thermally fatigues the $\emptyset$ 0.25 mm zinc-coated brass wire resulting in premature wire failure.

- **Secondary parameters influence:** Basic pulse parameters determine the theoretical spark ability, whereas secondary parameters govern the stability and physical efficiency of the interelectrode gap. The open and highly stable gap obtained with increased servo voltage to $S_v = 30$ V and accelerated wire feeds ($W_f = 7 - 12$ mm/min) improves the debris evacuation and suppresses the destructive arcing. In contrast, process retardation due to low settings ($S_v = 17$ V, $W_f = 3$ mm/min) results in a significant reduction in productivity.

- **Industrial recommendations for process continuity:** For the industrial production, where continuous execution is important, an optimized stable window of parameters is suggested: $T_{on} = 22 - 23\ \mu s$, $T_{off} = 33 - 35\ \mu s$, $S_v = 28 - 30$ V, and $W_f = 10 - 12$ mm/min. This configuration reduces the duty cycle to a dependable 38 – 40% range, maintaining 70 – 75% of peak productivity but preventing wire failure.

- **Surface integrity mitigation strategy**: Untempered martensite transformation creates a brittle, micro crack-prone recast layer (15 to 30 µm thick) from high-energy roughing passes. Two pass processing strategy is required for cyclic loaded components like EN31 bearing races. A high duty setting, fast roughing pass should be immediately followed by a precise finishing pass at conservative levels to remove the recast zone and to maintain structural integrity.

References

[1] R. M'Saoubi *et al.*, "High performance cutting of advanced aerospace alloys and composite materials," *CIRP Annals*, vol. 64, no. 2, pp. 557–580, Jan. 2015, doi: 10.1016/J.CIRP.2015.05.002.

[2] K. Lal and R. Trehan, "A review of tool wear and its effect on surface integrity of Inconel 718," *Machining Science and Technology*, vol. 30, no. 2, pp. 213–290, Dec. 2025, doi: 10.1080/10910344.2025.2598301.

[3] G. Mustafa, M. T. Anwar, A. Ahmed, M. Nawaz, and T. Rasheed, "Influence of Machining Parameters on Machinability of Inconel 718—A Review," *Adv. Eng. Mater.*, vol. 24, no. 10, Oct. 2022, doi: 10.1002/ADEM.202200202.

[4] L. Li, Z. Y. Li, X. T. Wei, and X. Cheng, "Machining Characteristics of Inconel 718 by Sinking-EDM and Wire-EDM," *Materials and Manufacturing Processes*, vol. 30, no. 8, pp. 968–973, Aug. 2015, doi: 10.1080/10426914.2014.973579.

[5] L. Slătineanu, O. Dodun, M. Coteaţă, G. Nagîţ, I. B. Băncescu, and A. Hriţuc, "Wire electrical discharge machining—a review," *Machines*, vol. 8, no. 4, pp. 1–28, Dec. 2020, doi: 10.3390/MACHINES8040069.

[6] C. Sarala Rubi *et al.*, "Comprehensive review on wire electrical discharge machining: a non-traditional material removal process," *Front. Mech. Eng.*, vol. 10, p. 1322605, Jan. 2024, doi: 10.3389/FMECH.2024.1322605/FULL.

[7] A. Payla, K. Chopra, and E. K. Mussada, "Investigations on power consumption in WEDM of EN31 steel for sustainable production," *Materials and Manufacturing Processes*, vol. 34, no. 16, pp. 1855–1865, Dec. 2019, doi: 10.1080/10426914.2019.1683577.

[8] M. Ehsan Asgar and A. K. Singh Singholi, "Parameter study and optimization of WEDM process: A Review," *IOP Conf. Ser. Mater. Sci. Eng.*, vol. 404, no. 1, p. 012007, Aug. 2018, doi: 10.1088/1757-899X/404/1/012007.

[9] S. Biswal, S. Tripathy, and D. K. Tripathy, "OPTIMIZATION OF WIRE EDM PROCESS PARAMETERS FOR EN-31 STEEL," *Optimization of Advanced Manufacturing Processes*, pp. 243–257, Jan. 2024, doi: 10.1201/9781003487128-14/OPTIMIZATION-WIRE-EDM-PROCESS-PARAMETERS-EN-31-STEEL-SMRUTIRANJAN-BISWAL-TRIPATHY-TRIPATHY.

[10] D. Mohanty and N. Nayak, "Effect of Process Parameters on Performance of EN-31 Steel using WEDM: Experimentation and Optimization," *International journal of engineering research and technology*, vol. V5, no. 07, Jul. 2016, doi: 10.17577/IJERTV5IS070291.

[11] S. Sharma, U. K. Vates, and A. Bansal, "Parametric Optimization of EN-31 Steel in Wire Cut Electro Discharge Machining by Taguchi Technique," *Adv. Sci. Eng. Med.*, vol. 12, no. 7, pp. 881–887, Dec. 2020, doi: 10.1166/ASEM.2020.2645.

[12] V. Sharma and S. H. A. Rizvi, "Investigation of parameters of Wire-EDM of EN-31 for Material Removal Rate and Surface Roughness," 2017.

[13] R. Kamalakannan, G. M. Pradeep, T. NaveenKumar, and M. Elango, "Machining parameters in WEDM of EN31 steel using Taguchi technique optimization," *Mater. Today Proc.*, vol. 50, pp. 1781–1785, Jan. 2022, doi: 10.1016/J.MATPR.2021.09.196.

[14] K. Chopra, A. Payla, and E. K. Mussada, "Detailed Experimental Investigations on Machinability of EN31 Steel by WEDM," *Transactions of the Indian Institute of Metals 2019 72:4*, vol. 72, no. 4, pp. 919–927, Jan. 2019, doi: 10.1007/S12666-018-1552-0.

[15] A. Tajdeen, M. Wasim Khan, K. Kamal Basha, E. Sakthivelmurugan, and NeerajaKoppula, "Experimental investigation and optimization of EDM process parameters on EN31 steel using genetic algorithm," *Mater. Today Proc.*, vol. 64, pp. 821–827, Jan. 2022, doi: 10.1016/J.MATPR.2022.05.326.

[16] R. Santosh Kumar and A. B. Naik, "Optimization of Material Removal Rate and Surface Roughness for EN31 Steel in Wire-EDM Process," *International Journal of Science and Research*, vol. 5, pp. 2319–7064, 2013, Accessed: Sep. 12, 2026. [Online]. Available: www.ijsr.net

[17] Investigation of Cutting Rate in Wire Cut Electrical Discharge Machining with EN-31 Alloy Steel using Single Objective Taguchi Method. Accessed: Sep. 12, 2026. [Online]. Available: https://www.researchgate.net/publication/287608839_Investigation_of_Cutting_Rate_in_Wire_Cut_Electrical_Discharge_Machining_with_EN-31_Alloy_Steel_using_Single_Objective_Taguchi_Method